AFRL-SA-WP-TR-2018-0007

Determining Spinal Posture for Encumbered Airmen in Crewstations Using the Luna Positioning Sensor

Jennifer J. Whitestone, Jeffrey A. Hudson, Brian Rife

711th Human Performance Wing, Airman Systems Directorate, Human-Centered Intelligence, Surveillance, and Reconnaissance Division

April 2018

Final Report
for October 2015 to October 2017

Air Force Research Laboratory
711th Human Performance Wing
U.S. Air Force School of Aerospace Medicine
Aeromedical Research Department
2510 Fifth St., Bldg. 840
Wright-Patterson AFB, OH 45433-7913

NOTICE AND SIGNATURE PAGE

AFRL-SA-WP-TR-2018-0007 HAS BEEN REVIEWED AND IS APPROVED FOR PUBLICATION IN ACCORDANCE WITH ASSIGNED DISTRIBUTION STATEMENT.

//SIGNATURE//	//SIGNATURE//
DR. JAMES McEACHEN	DR. RICHARD A. HERSACK
CRCL Human Performance	Chair, Aeromedical Research Department

REPORT DOCUMENTATION PAGE

Form Approved
OMB No. 0704-0188

1. REPORT DATE ***(DD-MM-YYYY)***	**2. REPORT TYPE**	**3. DATES COVERED** ***(From – To)***
25 Apr 2018	Final Technical Report	October 2015 – October 2017

4. TITLE AND SUBTITLE

Determining Spinal Posture for Encumbered Airmen in Crewstations Using the Luna Positioning Sensor

5a. CONTRACT NUMBER
FA8650-12-D-6354

5b. GRANT NUMBER

5c. PROGRAM ELEMENT NUMBER

6. AUTHOR(S)

Jennifer J. Whitestone, Jeffrey A. Hudson, Brian Rife

5d. PROJECT NUMBER
15-109

5e. TASK NUMBER
FPH01.0002.0003.012.04 TO2

5f. WORK UNIT NUMBER

7. PERFORMING ORGANIZATION NAME(S) AND ADDRESS(ES)
711th Human Performance Wing
Airman Systems Directorate
Human-Centered Intelligence, Surveillance and Reconnaissance Division
Human Signatures Branch
Human Detection and Characterization Section
Wright-Patterson AFB, OH 45433-7947

8. PERFORMING ORGANIZATION REPORT NUMBER

9. SPONSORING / MONITORING AGENCY NAME(S) AND ADDRESS(ES)
USAF School of Aerospace Medicine
Aeromedical Research Dept/FHOH
2510 Fifth St., Bldg. 840
Wright-Patterson AFB, OH 45433-7913

10. SPONSORING/MONITOR'S ACRONYM(S)

11. SPONSOR/MONITOR'S REPORT NUMBER(S)
AFRL-SA-WP-TR-2018-0007

12. DISTRIBUTION / AVAILABILITY STATEMENT

DISTRIBUTION STATEMENT A. Approved for public release. Distribution is unlimited.

13. SUPPLEMENTARY NOTES
Cleared, 88PA, Case # 2018-2707, 25 May 2018.

14. ABSTRACT
A major thrust of the U.S. Air Force anthropometric engineering mission is to develop analytical and statistical tools to be applied to the databases to characterize design-relevant body size and shape variation as it applies to our service personnel. Of particular interest is cockpit accommodation using subjects representing variability in body size and equipped with aircrew flight equipment including helmet systems, protective equipment, survival gear, restraints, and flight clothing. This equipped human subject pool is used to "map" the accommodation issues and "train" the human figure models to reproduce their size, proportions, and performance. Essentially, this mapping process links the anthropometry of the subjects to their performance in the mockups. Through regression analysis, resulting maximum and minimum anthropometric values are quantified and used to determine accommodation levels (percentage accommodation) during normal and emergency operation and if requirements are met. Of importance is the fidelity of the models used to assess accommodation. As such, the anthropometric engineering team continues to improve data collection methods and modeling techniques to build confidence in virtual assessments. For this effort, the Luna, Inc. fiber optic positioning sensor was evaluated to determine the utility of this lightweight, miniature technology to track spine posture and position. Results show that the Luna fiber optic sensor will make an excellent tool to collect spinal posture data that will increase the fidelity of our digital human figure modeling as well as biodynamic modeling.

15. SUBJECT TERMS
Anthropometry, spinal posture capture, comfort, fatigue, injury risk assessment comfort, workstation design

16. SECURITY CLASSIFICATION OF:			**17. LIMITATION OF ABSTRACT**	**18. NUMBER OF PAGES**	**19a. NAME OF RESPONSIBLE PERSON**
a. REPORT	**b. ABSTRACT**	**c. THIS PAGE**			Domonique Chapa
U	U	U	SAR	34	**19b. TELEPHONE NUMBER** ***(include area code)***

This page intentionally left blank.

TABLE OF CONTENTS

Page

LIST OF FIGURES ii
LIST OF TABLES ii
1.0 SUMMARY 1
2.0 INTRODUCTION 1
2.1 Evaluation of Digital Human Modeling 2
2.2 RAMSIS NextGen Digital Human Model 3
2.3 Background on Luna Technology 6
2.4 Impact on Pilot Safety 7
3.0 METHODS, ASSUMPTION, AND PROCEDURES 8
3.1 Luna Measurement System 8
3.2 3DMD Whole Body Scanner 9
3.3 Artec Eva Handheld Scanner 9
3.4 Polyworks 10
3.5 RAMSIS NextGen DHM Posture Driver 10
3.6 Data Collection 12
3.6.1 Evaluation using Artec Eva Handheld Scanner 12
3.6.2 Evaluation Using 3DMD Whole Body Scanner 14
3.6.3 Evaluation Using Human Solutions VITUS Whole Body Scanner 17
4.0 RESULTS AND DISCUSSION 19
5.0 CONCLUSION 19
6.0 REFERENCES 20
APPENDIX – Results of 3DMD Evaluation of Luna Positioning Sensor 21
LIST OF ABBREVIATIONS AND ACRONYMS 28

LIST OF FIGURES

Page

Figure 1. Capturing reach data 4
Figure 2. Generating a reach cell 4
Figure 3. The RAMSIS NextGen model 5
Figure 4. Scan of large subject (near case 5) in ACES II seat aligned with the CAD cockpit, seat in the full down position 5
Figure 5. Luna orientation and posture TRACking system as developed under the Test Resource Management Center Test and Evaluation/Science & Technology Program through the U.S. Army Program Executive Office for Simulation, Training and Instrumentation 6
Figure 6. Demonstration of "crash" posture 7
Figure 7. The technology behind the Luna fiber optical positioning device 8
Figure 8. The 3DMD whole body scanner 9
Figure 9. RAMSIS models developed from PCA dimensions and scans of subjects most closely representing each case 11
Figure 10. Estimation of vertebral locations 11
Figure 11. Initial evaluation of the Luna positioning sensor 12
Figure 12. Surface scan acquired using the Eva scanner and Luna output 14
Figure 13. Performance of the Luna sensor with and without encumberment 14
Figure 14. Luna sensor evaluation conducted with 3DMD whole body scanner 15
Figure 15. Example of a data quality plot for the subject's posture 16
Figure 16. Implementation of Luna system to capture initial posture 18

LIST OF TABLES

Page

Table 1. Transformation from Sensor Coordinate System to Customer-Preferred Alignment ... 13
Table 2. An Example of a .csv File Used as Output from the Luna Sensor for One Posture 16
Table 3. Results of the Coordinate Data Extracted from 3DMD Scans Using Polyworks vs. the Luna Sensor Output 17

1.0 SUMMARY

A major thrust of the U.S. Air Force anthropometric engineering mission is to develop analytical and statistical tools that can be applied to existing databases to characterize design-relevant body size and shape variation in our service personnel. Of particular interest is the "mapping" of pilot physical accommodation space in the cockpit environment. To execute their mission, pilots have very defined functional requirements related to vision in and out of the cockpit, reaching and operating controls, and staying clear of obstructions throughout normal flight operation as well as during emergency egress. To construct accommodation envelopes, we use test participants representing variability in body size equipped with aircrew flight equipment, which includes helmet systems, protective equipment, survival gear, restraints, and flight clothing. This equipped human subject pool is used to map the accommodation issues and define body size parameters needed to fly their mission safely.

Essentially, during data analysis, the live subject mapping process links the anthropometry of the subjects to their performance in the mock-ups. Statistical analysis of the data results in minimum and maximum anthropometric values, which are used to determine accommodation levels (percentage accommodation) via virtual fit testing of a user representative database. For acquisition programs, these are the same results used to determine if requirements are met by a vendor design. The live subject data are also used to "train," or increase the fidelity of, digital human figure models, which are integral in the computer-aided design process for cockpits and workstations. Clearly, any improvements that can be made to test participant data collection produce more accurate accommodation estimates as well as better digital human modeling algorithms. As such, the anthropometric engineering team constantly strives to improve data collection methods and modeling techniques to build confidence in virtual assessments.

For this effort, the Luna, Inc. fiber optic positioning sensor was evaluated to determine the utility of this lightweight, miniature technology to track spine posture and position. The approach to acquiring spinal posture data for improved digital human modeling required the 3DMD whole body scanning system, the Artec EVA handheld scanner, RAMSIS NextGen digital human model, Human Solutions VITUS whole body scanner, and a Luna, Inc. fiber optic cable. A subject posing in various upper body postures while wearing the Luna positioning sensor was used to gather data simultaneously using both the Artec EVA and the 3DMD. Coordinate data extracted from the 3DMD scans were compared to the positions of identical points along the spine recorded using the Luna system. The resulting positional error standard deviations never exceeded 2 mm. The Luna fiber optic sensor will make an excellent tool to collect spinal posture data that will increase the fidelity of our digital human figure modeling as well as biodynamic modeling.

2.0 INTRODUCTION

Anthropometric engineering (AE) for the U.S. Air Force (USAF) serves to support both research and development and Program Offices with acquisitions and modifications to aircraft, ground vehicles, protective equipment, clothing, and other equipment that must interface with the human body. Major functions of AE include developing and maintaining anthropometric databases, developing analytical and statistical tools to be applied to the databases to characterize design-relevant body size and shape variation of our service personnel, and supporting USAF

programs by supplying data and expert analyses on physical accommodation. Anthropometric data (human body measurements) are acquired using both traditional tools, such as calipers and tape measures, and surface scanning technologies, such as three-dimensional (3D) digitizers, whole body scanners, and handheld sensors. These measurement data can be collected as part of a population survey or individual data from an accommodation evaluation. In the case of accommodation evaluations, AE relies on subjects measured in actual cockpits and workstations to estimate the percentage of body size and shape accommodation [1]. This approach provides quantification of how small, big, and anthropometrically proportioned an operator can be and still safely and effectively perform the mission.

Of critical importance is seated posture. Accurate postural data are significant for defining the starting position for modeling human performance and spinal loading, both in normal operation as well as loading during high-G maneuvers and aircraft ejection. Back pain issues have been documented in bomber pilots due to asymmetric postures required for their mission. Additionally, pain has been reported for long sorties in aircraft such as the B-1 and F-16. Currently, posture is derived from high-resolution whole body surface scans of the body's surface or, even more inaccurately, from the equipped subject where the posture can only be inferred. Using Luna's newly developed positional measurement system, a fiber optic cable that is secured directly to the subject's back beneath their clothing, the vertebral positions can be recorded relative to the whole body position. Spine posture data can be acquired to provide valuable human modeling information needed to realistically represent spinal location and orientation for development and evaluation of equipment and operator environment. Hence, our goal was to develop the methodology to capture spinal posture and integrate these data with current surface scanning capability.

2.1 Evaluation of Digital Human Modeling

Gathering empirical subject data within a cockpit environment is necessary to quantify accommodation and determine body size limitations [1]. Digital human modeling (DHM) software is also useful for understanding accommodation; however, it is generally used as a visualization tool, not as an analytical tool, as the models have not been reliable. In fact, during the Joint Primary Aircraft Training System (JPATS) T-6A acquisition program, it became clear that DHM systems were unverified and unvalidated, and could not be used to estimate cockpit accommodation [2]. To demonstrate accommodation, one vendor relied on a DHM and claimed a particular level of accommodation. However, the digital manikin results were in error of up to 4 inches on some anthropometric dimensions. As a result, the USAF AE team and TNO Defence, Security and Safety (Business Unit Human Factors) evaluated five commercial DHM systems. There were two phases: 1) anthropometric verification of the manikins and 2) comparing the accommodation limits offered by the DHM in an F-16 fighter computer-aided design (CAD) model against the accommodation limits of an actual F-16 fighter obtained by using human subjects. The study revealed that none of the DHMs could be reliably used for evaluations [2]. Furthermore, it was determined that baseline information on initial pilot position and posture, soft tissue compression, seat cushion effects, restraint harness effects, and protective ensemble effects must be established within each DHM. Other studies have also demonstrated that the fidelity of a DHM can be significantly improved by embedding subject performance data as input parameters [3-5].

To this end, the USAF AE team used subjects of various size and shape to collect position, posture, and performance data with 3D scanners. The subjects, while wearing aircrew flight equipment (AFE) appropriate for the seat of interest, were measured for reach, vision, and clearance while seated in specific aircraft/operator workstation seats. The scanned posture and position data during reaches, for instance, cannot only be used to quantify differences in encumbering effects of competing gear but also can be used to "train" and improve the fidelity of DHMs. Figures 1 and 2 show a small subject equipped with AFE seated and restrained in an ejection seat and electronically captured while performing reaches. In this example, it is evident that the resulting reach "shell" is reduced due to the AFE. Ultimately, improving the models will help to provide the USAF with the ability to conduct accommodation analyses based on verified DHM systems, particularly on simple cockpit modifications, in lieu of expensive live subject studies.

2.2 RAMSIS NextGen Digital Human Model

The USAF AE team has adopted the Human Solutions RAMSIS NextGen DHM (Rechnergestütztes Anthropometrisch-Mathematisches System zur Insassen-Simulation) as a platform upon which to build biofidelic digital manikins. RAMSIS NextGen is a modeling and simulation software tool that provides a digital library of human body shape, reach, posture, and performance. RAMSIS NextGen includes baseline CAD software for generating cockpit environments as well as an extensive database of representative body dimensions. The USAF AE team is working toward validating and verifying RAMSIS NextGen, which includes fidelity improvements from live subject data, such that it will provide simulation of pilots in a cockpit environment to represent reliable scenarios.

The RAMSIS model comprises two structures that represent the manikin. These include an inner linkage system representing a simplified skeletal structure and the outer skin representing the body's surface. Figure 3 shows an example manikin with the linkage system (a) and outer skin represented with a wireframe (b) that is enfleshed as shown in (c). The deformable "skin" allows for realistic representation of contact between the subject and equipment or seat structures. The manikin can be "seated" by manipulating segments and assigning joint angles.

While the RAMSIS NextGen model does provide an initial *pilot* posture, this posture has not been verified. Early development of the pilot posture model was conducted by Kaibel et al. using cameras to capture actual pilot subjects in various postures such as takeoff, climb, cruise, descent, and landing [6]. The RAMSIS manikin was superimposed on the pilot posture images, visually overlapping the surfaces of the two models. While the different postures were captured, such as takeoff versus climb, it is still imperative to determine the impact on pilot posture models with subjects of extreme body size, different seat geometries (particularly seat back angles), and the pilot's AFE. An additional ergonomic study by the automotive industry demonstrated that the posture prediction of the RAMSIS model was in error of 8.7° to 74.9° between RAMSIS predicted postures and those measured with a 3D digitizer for body segment locations and driving tasks [7].

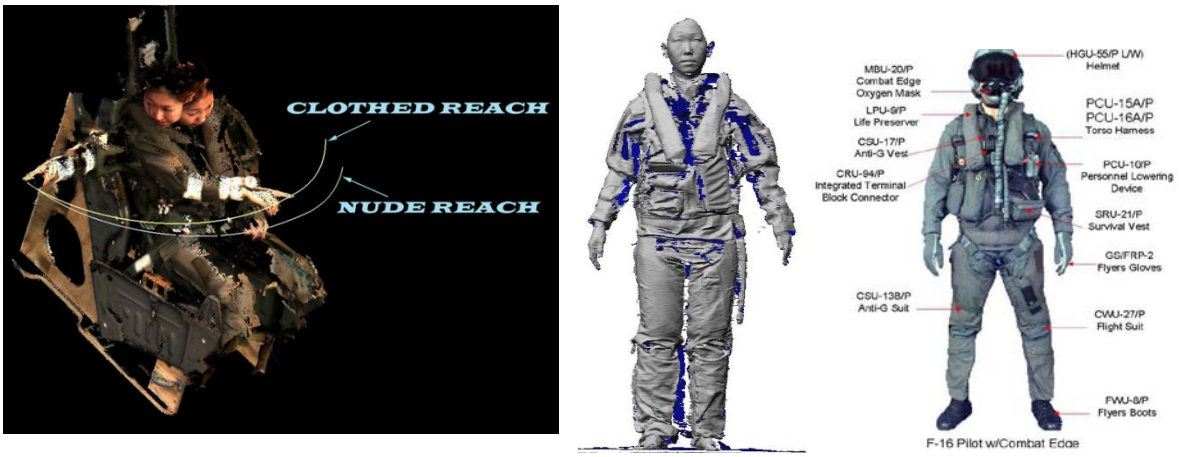

Figure 1. Capturing reach data. Capturing seat-specific reach data for a small subject reveals the reduction in reach capability due to multi-layered aircrew flight equipment as shown on the right.

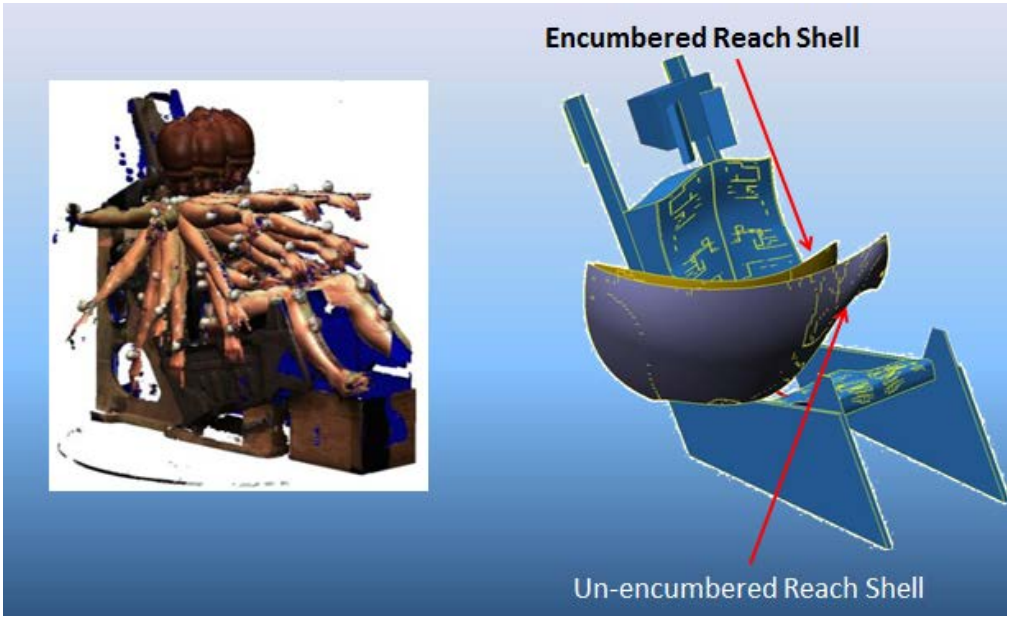

Figure 2. Generating a reach cell. Subjects are equipped with AFE and restrained in the ejection seat prior to performing reach operations, which are recorded using 3D surface scanning methods. Ultimately the reach points are used to generate a "reach shell," which demonstrates the maximum restrained reach for each subject and can be modeled in the DHM. As shown Figure 1, while wearing the AFE, the subject's reach radius is reduced. It is important to quantify the effect of particular AFE configurations on a subject's performance.

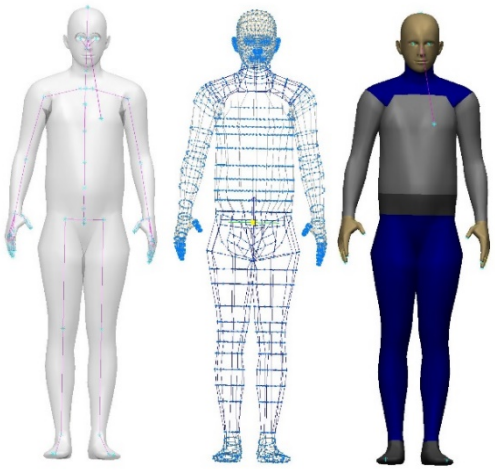

Figure 3. The RAMSIS NextGen model. This model offers a manikin that is made up of an inner linkage system (a) representing a simplified skeletal structure and an outer skin modeled as a wireframe (b) that can enfleshed (c).

RAMSIS NextGen DHM software does offer generalized body posture modeling capability. However, the posture algorithm must be validated using non-line-of-sight technology to measure spine orientation given a wide range of body size and aircrew seating/ equipment configurations. Establishing a realistic posture model is critical to modeling position for assessing reach and clearance in vehicles and cockpits. As such, the USAF AE team is currently acquiring deliberate and appropriate human body posture and position data, specific to body size, ejection/cockpit seat, and encumberment. Shown in Figure 4 is a "large" subject scanned in ejection seat posture next to a "large" RAMSIS manikin registered with the subject data. The surface registration approach is a first step in establishing seat-specific postures, but provides external surface data only. Being able to collect position and posture data on the body segments below the personal gear would dramatically improve placement of the RAMSIS linkage system. To this end, the application of the Luna positioning sensor to acquire spine posture will fulfill the requirement for vertebral alignment as input to the model.

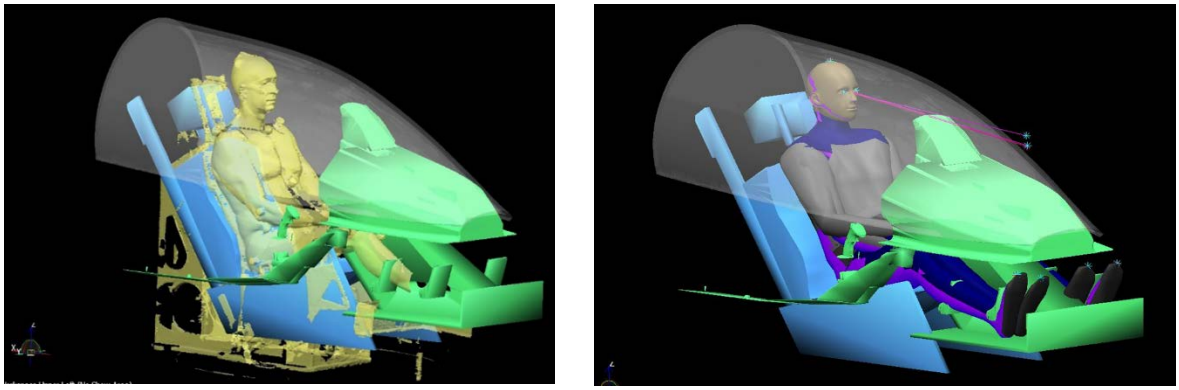

Figure 4. Scan of large subject (near case 5) in ACES II seat aligned with the CAD cockpit, seat in the full down position. A RAMSIS manikin generated (and verified) with the anthropometry of the large subject is visually matched to the scan. This subject manikin joint angle posture file is saved.

2.3 Background on Luna Technology

Luna, Inc. (Blacksburg, VA) has developed, and is refining, an innovative non-line-of-sight wearable fiber optic-based technology (Luna TRAC system) that is intended to provide soldier orientation and posture data for U.S. Army field-based research programs. Real-time shape and position data are generated through measurement of strain (axial twist and curvature) in the helically twisted optical cables that lie inside the length of the sensor via optical frequency domain reflectometry technology. This sensor system has negligible weight and no impact on equipment fit or subject performance. While other types of bend sensor platforms exist (e.g., resistor-based from Flexpoints Sensor Systems), the TRAC system is already under development for Department of Defense applications and was available for evaluation. The Luna fiber optic system is under development by the Test Resource Management Center to build a full-body system for the dismounted soldier as shown in Figure 5. While preparing for the Army Test and Evaluation Command evaluations, Luna identified a single-sensor, benchtop version of the full-body system, which was used for our application.

Figure 5. Luna orientation and posture TRACking system as developed under the Test Resource Management Center Test and Evaluation/Science & Technology Program through the U.S. Army Program Executive Office for Simulation, Training and Instrumentation.

The need to accurately acquire and record spine location given various seated postures of the equipped operator is not unique to the USAF. In fact, the USAF AE team is part of a multiservice anthropometric working group, a coalition of experts working on different sensing technologies. In April 2016, the USAF AE team organized and participated in a multiservice Department of Defense and academia workshop on DHM for long-term planning and sharing of anthropometric resources. Of interest in the discussion is the collaboration to develop improved head/neck spine modeling. The USAF's efforts applying the Luna system to seat-specific posture modeling as input to the RAMSIS NextGen model have elevated the interest in the use of fiber optic positioning for the other services. For seat posture applications, the Luna system is ideally suited to a mounted environment where movement is considerably less than dismounted, with a place for the data collection laptop/tablet and adequate cooling so the additional garment that holds the fiber cable will not be a heat burden, and the full data output—position and shape—has direct relevance to behavior (i.e., controlling the aircraft).

2.4 Impact on Pilot Safety

Postural data are important in defining the starting position for modeling human performance and spinal loading, both in normal operation as well as loading during high-G maneuvers and aircraft ejection. Currently, posture is derived from high-resolution whole body surface scans of the body's surface or, even more inaccurately, from the equipped subject where the posture can only be inferred. An example of the use of 3D sensors, such as the Artec Eva (Santa Clara, CA) and Kinect handheld scanners (Microsoft, Redmond, WA), to acquire body position and posture is shown in Figure 6 as the pilot demonstrates a "crash" posture. Using Luna, a fiber optic cable that is secured directly to the subject's back beneath his or her clothing, the vertebral positions can be recorded relative to the whole body position. Spine posture data can be acquired to provide valuable human modeling information needed to realistically represent spinal location and orientation for development and evaluation of equipment and operator environment. Hence, it is important to develop a methodology to capture spinal posture and integrate these data with current surface scanning capability.

Figure 6. Demonstration of "crash" posture. On the left, the pilot is demonstrating a "crash" posture, which is captured on the right using handheld scanners (Artec Eva and Kinect).

Aircrew posture and orientation differ depending on the configuration of the pilots' seating system/workstation and the encumbrance of their protective equipment. In addition, loading forces from the external environment, as well as from donned equipment, change as a factor of body orientation. The products of this research directly relate to aircrew safety, health, and survivability issues that align with the Air Force Medical Service Strategy Map 3.0, i.e. "Ensure medically fit forces … and improve the health of all we serve to meet our Nation's needs." Additionally, there has been concern that the small female pilot may experience different dynamic response, particularly in specific ejection seats. Capturing spine and whole body posture in the ejection seat will allow for estimation of whole body center of gravity (CG) for specific subject size. Whole body CG location is required to model the subject's biodynamic response.

The AE team has used digital human body modeling systems in the past, but as visualization tools and not as analytical tools. Given the capability and specificity of modeling using RAMSIS, as well as accurately collecting spine posture using Luna given various seated postures and equipment, it will be possible to develop predictive capability for operators within cockpits and workstations. Furthermore, capturing and modeling body posture data of small pilots can assist in determining the impact of whole body CG prior to ejection scenarios. Working with USAF biodynamic engineers on ejection seat impact, these data will refine current biodynamic simulations.

3.0 METHODS, ASSUMPTION, AND PROCEDURES

The approach to acquiring spinal posture data for improved DHM required the 3DMD whole body scanning system, the Artec Eva handheld scanner, RAMSIS NextGen DHM, and a Luna fiber optic cable. A subject posing in various upper body postures while wearing the Luna positioning sensor was used to gather data simultaneously using both the Artec Eva and the 3DMD. Coordinate data extracted from the 3DMD scans were compared to the positions of identical points along the spine recorded using the Luna system. The RAMSIS NextGen DHM is not programmed to automatically input vertebral locations from the human spine to the model. The model's spine orientation engine was studied to determine the most direct method of inputting the Luna data. An approach was developed to translate Luna data to drive the RAMSIS spine model.

3.1 Luna Measurement System

Luna, Inc. provided a prototype single fiber cable for the evaluation conducted using the 3DMD whole body scanner located at Wright-Patterson Air Force Base. Luna's shape-sensing technology can track the position (location) of an optical fiber to a high degree of accuracy along its entire length. This "smart fiber" is minimally intrusive, virtually weightless, and can be used to monitor the dynamic 3D shape of a structure to which it conforms. The unique helical, 4-core optical fiber measures strain on each core, converting the data to 3D shape as shown in Figure 7. Data were collected using a G4 OPAL fiber optic shape sensor and interrogation instrument.

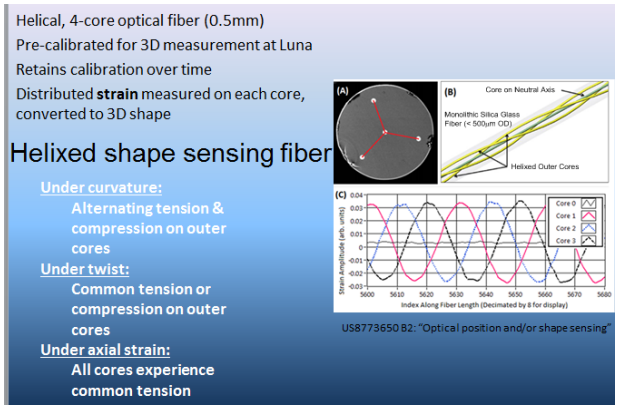

Figure 7. The technology behind the Luna fiber optical positioning device. The unique helical, 4-core optical fiber measures strain on each core, converting the data to 3D shape.

3.2 3DMD Whole Body Scanner

Evaluation of the Luna fiber optic positioning method requires the use of an independent coordinate measurement system. The 3DMD scanners are used to obtain 3D images and models of an individual body part or the entire human body without safety risk to people and magnetic radiation and with no need for special markers. The 3DMD scanners use PerkinElmer xenon flash tubes (Waltham, MA) mounted inside metal cases with a reflector to direct light toward the subject. The light is either diffused through a polycarbon filter or projected through a glass slide that contains a random speckle pattern. The amount of light produced by the flash is similar to that generated by a flash in an off-the-shelf camera. The maximum flash energy is 11.3. The continuum is very similar to sunlight (7000K).

The 3DMD whole body 18-camera scanner was implemented for the study of a subject while wired with the Luna system attached to his spine. The 3DMD scanner is a one-of-a-kind scanning volume comprising 18 pods containing both geometric and radiometric sensors to capture surface data of subjects along with aligned texture information (Figure 8a). A surface scan and the scan with color texture-mapped to the range data are shown in Figure 8b.

(a) (b)

Figure 8. The 3DMD whole body scanner. (a) This scanner has only 8 pods, while the 3DMD system used by the USAF has 18 scanning pods for improved resolution and greater scanning volume. (b) Subject scan data showing both geometry and texture data.

3.3 Artec Eva Handheld Scanner

The Artec Eva scanner uses white light technology similar to regular cameras and captures thousands of measurements in seconds. The scanners have been on the market, used throughout the world, for more than 7 years scanning human faces without incident. The Artec scanner does not contain any lasers and is absolutely safe for eyes and skin. The average output power is not more than 0.5 mW/cm^2 (distance from the scanner – 640 mm). The peak power (impulse ~200 µs) is 165 mW/cm^2 (distance from the scanner – 640 mm). The flash operates for 0.2 ms once every 66.4 ms. The flash, standard xenon flash tube with glass type B, is in the infrared part of the spectrum less than 20%. The Eva scanner is handheld and the operator directs the imaging device along the surface of interest, capturing images at approximately 15 Hz.

3.4 Polyworks

Polyworks (InnovMetric Software Inc.) is regularly employed by all members of the AE team as a powerful image software editing and quantification tool for projects related to protective equipment as well as cockpit design and evaluation. Polyworks' advanced image processing algorithms allow anthropometrists to quickly and easily translate point cloud data to surface models for measurement or replication purposes either within Polyworks or for other CAD programs. Polyworks offers the ability to develop command line scripts to reduce post-processing time. Polyworks also provides data acquisition modules for the portable surface digitizing systems used in the lab including both FARO arms and 3DMD. Surface models from Polyworks can be directly imported to RAMSIS to drive human body modeling.

3.5 RAMSIS NextGen DHM Posture Driver

RAMSIS provides a sophisticated ergonomic simulation environment that has been co-developed and tested by leading automotive industry partners, with an interest in modeling interior accommodation and providing for safety in the dynamic environment. Human Solutions also has a long-standing partnership with the U.S. Army, which uses RAMSIS for product development. The software benefits from the largest international body dimensions database with more than 100,000 subjects. RAMSIS technology represents models that reflect a combined expertise in anthropometry, ergonomics, statistics, simulation, visualization, and virtualization. Various methods of representing body models include grid, surface, physiological joint location, and simulation. RAMSIS also offers automatic posture calculation, motion and force analysis, reach analysis, integration of standards, direct visibility analysis, calculation of maximum postural force (hand-arm system), motion recorder, and compatibility with 3D body scanners.

The AE team relies on a multivariate method, or principal component analysis (PCA), to specify pilot body size for anthropometric accommodation in USAF cockpit designs. PCA describes the variation of the original multivariate distribution with a set of orthogonal axes (principal components) and acts to reduce a large population database to select body types that represent variability [8]. Selection of the anthropometric measurements, the number of principal components used to represent the variation in their distribution, and a full understanding of the assumptions implicit in the model are all critical in generating useful representative accommodation cases [9]. PCA models that represent variability in body size as it relates to cockpits use only six dimensions as input known as the "cockpit six." Development of the PCA models within RAMSIS was problematic, as the anthropometric engine did not produce manikins directly proportional to the dimensional input, particularly given only six dimensions. Initially, the basic "Typology" manikin generating function was used in an attempt to create RAMSIS manikins that represented measured subjects. A number of errors and software bugs in the anthropometric engine of NextGen version 1.2 were found and reported to the software developer Human Solutions (Germany), resulting in an updated "Body Builder Pro" anthropometric input engine. In addition to this update, an iterative input method was developed by the AE team to produce manikins that directly represented the anthropometric input. To ensure an acceptable level of accuracy with manikin representation, the USAF multivariate cases (cases 1-9) were created and anthropometric measurements compared to original input. To supplement the anthropometric dimensional input (beyond the cockpit six), "nearest neighbors" from the Aircrew Sizing Survey as well as U.S. Army subjects from ANSUR II were identified

to serve as target values for additional measurements extracted from RAMSIS NextGen. Figure 9a shows cases 1-9 as RAMSIS models developed from the PCA dimensions and Figure 9b are scans of subjects whose dimensions most closely represent each case.

(a) (b)

Figure 9. RAMSIS models developed from PCA dimensions and scans of subjects most closely representing each case. (a) From the left, JPATS 1-7, Joint Strike Fighter (JSF) 8, and KC-X 9 as final RAMSIS manikins represent the 3D manifestation of the tabled multivariate case values. (b) Shown on the right are selected nearest neighbors closest to JPATS 1-7, JSF 8, and KC-X 9 used to improve the fidelity of the 3D RAMSIS multivariate cases.

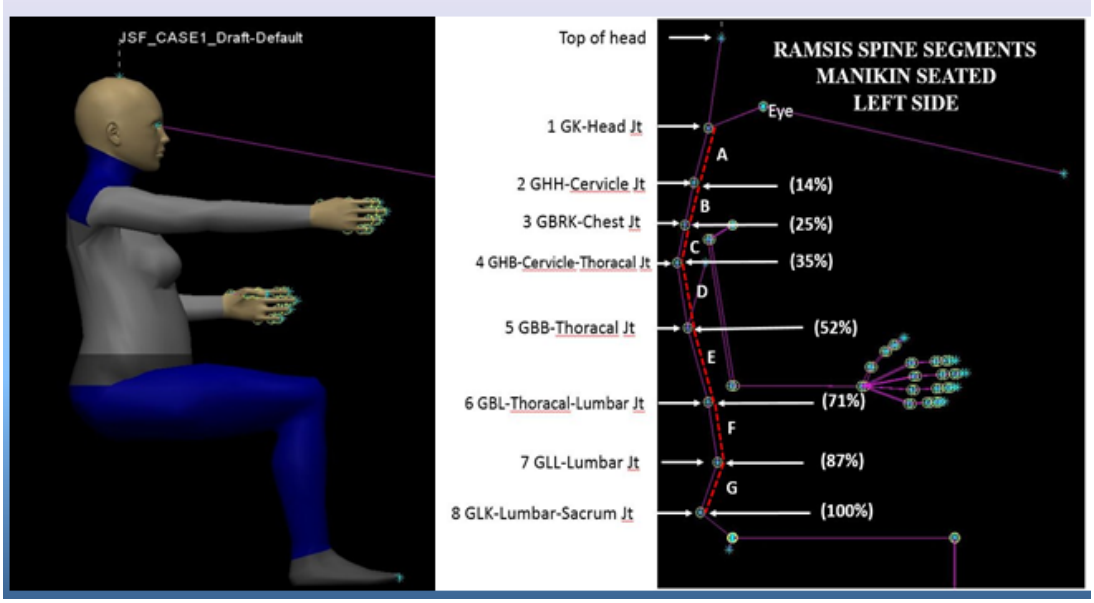

Figure 10. Estimation of vertebral locations. A small RAMSIS manikin is seated and the vertebral element locations are estimated along the skeletal model.

Now that the manikins can be established from anthropometry, the vertebral model must be realistically represented. The location for each vertebra, however, is not directly called out in the skeletal model of the RAMSIS manikin. Therefore, using a small and large subject, an estimation of the vertebral locations was determined as a percentage of spine length. It is speculated that the spinal locations can be further refined by using the Luna positioning sensor. In Figure 10, a seated small subject shown enfleshed and clothed on the left is positioned using the skeletal structure within the manikin. An approximation of vertebral elements is assigned to the skeletal spine and used to rotate the manikin into a seated posture.

3.6 Data Collection

3.6.1 Evaluation using Artec Eva Handheld Scanner. The initial evaluation of the Luna positioning sensor, using the Artec Eva handheld scanner, was conducted at the Luna, Inc. facility in Blacksburg, VA. A single fiber optic cable was packaged in a 0.9-mm-diameter polyvinyl chloride tube and threaded through Luna's shape-sensing body suit worn by a Luna employee. The shape sensor was routed in a U-shaped configuration on either side of the spine, with the apex fixed near the C7 vertebra, as shown in Figure 11a. The sensor's aluminum coordinate reference box was mounted on a 3D-printed belt mount, which was in turn attached to the test subject's belt. All data were collected with the egress of the sensor (Z-axis of the coordinate system) facing downward. A reference point was chosen on the floor of the reference box's 3D-printed enclosure at the upper left corner (Figure 11b). After testing was completed, but before sensor disassembly, Luna recorded coordinate offsets between the shape sensor's measurement coordinate frame and the chosen reference point.

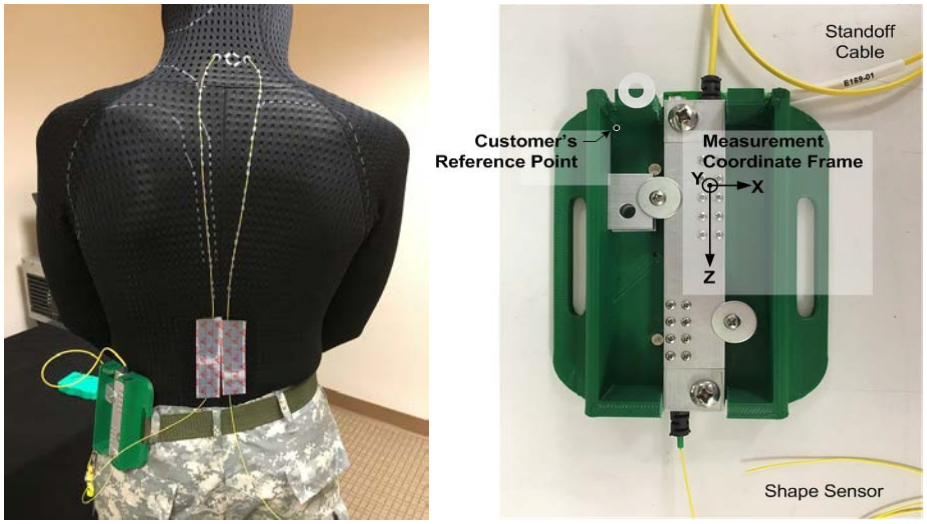

(a) (b)

Figure 11. Initial evaluation of the Luna positioning sensor. (a) Subject wearing the shape-sensing body suit with a single sensor woven in a U-shape along either side of the spine. (b) The data were collected via the data acquisition box mounted on the subject's belt.

It is important to note that the coordinate offsets were computed relative to the sensor's default measurement frame, in which the X-axis runs along the floor of the sensor's aluminum reference box and the Y-axis is normal to the floor of that reference box. This coordinate frame was achieved with a sensor initial roll setting of 4.21 radians. During testing, the coordinate system was manually rotated about the Z-axis to an initial roll setting of 0.691 radians. This rotation was performed to bring the sensor in alignment with the plane of the test subject's back. Table 1 shows the reference distances to align the fiber with the acquisition box coordinate system to permit comparison of the sensor against the Eva scans of the same surface.

Table 1. Transformation from Sensor Coordinate System to Customer-Preferred Alignment

Coordinate	ΔR(a) Sensor Origin to Reference Box Offset (mm)	ΔR(b) Reference Box to Belt-Mount Offset (mm)	ΔR(c) Sensor Origin to Customer Reference Point (mm)
X	-6.5	48.0	41.5
Y	7.5	0.0	7.5
Z	47.8	-7.0	40.8

ΔR(a) = location of sensor origin – location of ref box corner. ΔR(b) = location of reference box corner – location of customer reference. ΔR(c) = location of sensor origin – location of customer reference point.

While the positioning data were recorded by the Luna shape-sensing fiber, the subject was scanned with the Artec handheld scanner. Data from both sensors were collected with the test subject statically holding eight different positions. In each position, 50 shape-sensing measurements were logged in rapid succession as the subject was scanned. The G4 shape-sensing interrogator collects data at 250 Hz; each data log represents 200 ms worth of measurement data. A surface scan acquired using the Eva scanner is shown in Figure 12a. In this example, the subject is twisting left. The resulting Luna sensor data are shown as two planar projections of the movement (Figure 12b). The Eva scan data and Luna sensor results were aligned using Polyworks, and a distance map of the two surfaces shows differences less than 2 mm. This level of error was determined for all body postures collected using the Eva scanner.

Performance of the Luna sensor with the addition of encumberment such as body armor was evaluated using the Eva scanner, capturing the surface data of the subject with and without encumberment. The subject attempted to recreate all unencumbered movement such as leaning left, right, and forward while wearing the Luna sensor underneath the body armor. Although the Eva scanner cannot capture the shape of the subject's back with line-of-sight techology, the Luna positioning output data were similar to the unencumbered output and not impeded by the body armor. Figure 13 shows the subject leaning forward with and without body armor. The Luna positioning output data for each configuration demonstrate reliability of the Luna sensor.

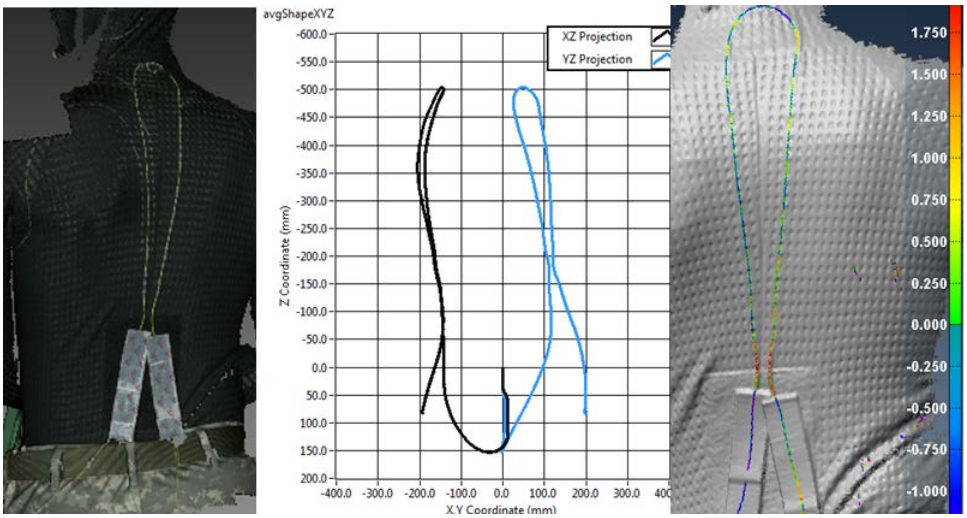

(a) (b) (c)

Figure 12. Surface scan acquired using the Eva scanner and Luna output. (a) An Eva scan of the subject twisting left with the sensor output (b) showing the position of the subject's back. (c) Alignment of the Eva surface data with the Luna sensor output using Polyworks demonstrates a surface distance within a 1- to 2-mm error, well within the tolerance of spine measurement required for posture location application.

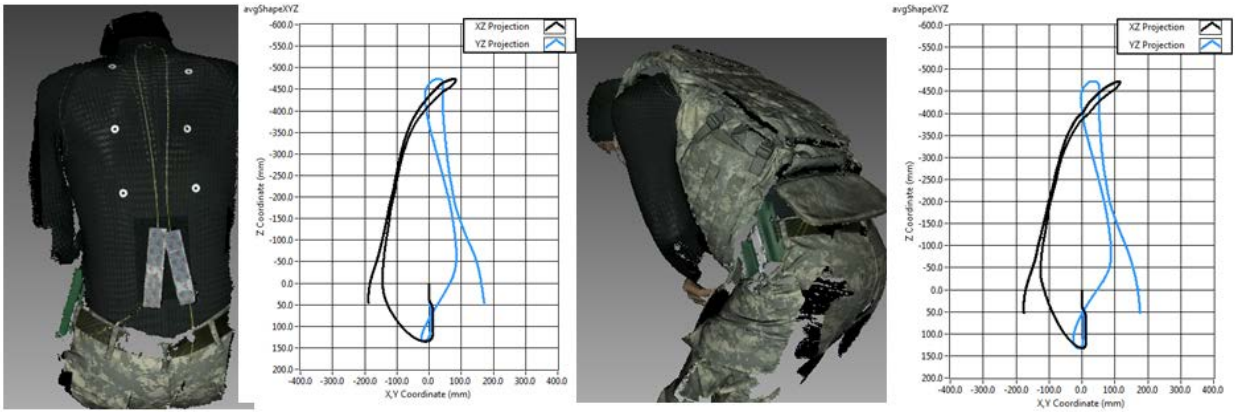

(a) (b)

Figure 13. Performance of the Luna sensor with and without encumberment. (a) Subject unencumbered and leaning forward. The Luna output from the positioning sensor along the spine is shown to the right of the scan image. (b) Same subject wearing body armor and leaning forward. The output data from the Luna sensor demonstrate the same posture output.

3.6.2 Evaluation Using 3DMD Whole Body Scanner. A second evaluation of the Luna sensor was conducted with the 3DMD whole body scanning system. A male subject was outfitted with scanning shorts, and the Luna fiber optic cable was secured along his spine as shown in Figure 14a. Points along the spine, and Luna cable, were marked with fiducials as shown. A 3D textured scan of the patient standing straight is shown in Figure 14b with the Luna system visible in the scan data. As the Luna system provides continuous positioning coordinate data along the length of the fiber, specific points along the fiber that corresponded to points on the spine were identified using the "cold touch" method. A canister of compressed air was turned upside down

to release a cold liquid. As the gases are compressed to liquid form, when the can is turned upside down, liquid is released from the nozzle before it has a chance to convert to a gas. The Q-tip was used to place the cold liquid on targeted locations along the fiber optic cable, resulting in a spike in the measurement data as shown in Figure 14c. The subject was scanned using the 3DMD system while standing in the middle of the scanning volume and posing with various spine postures for each scan including standing straight, bending left and right, bending forward, and twisting left and right.

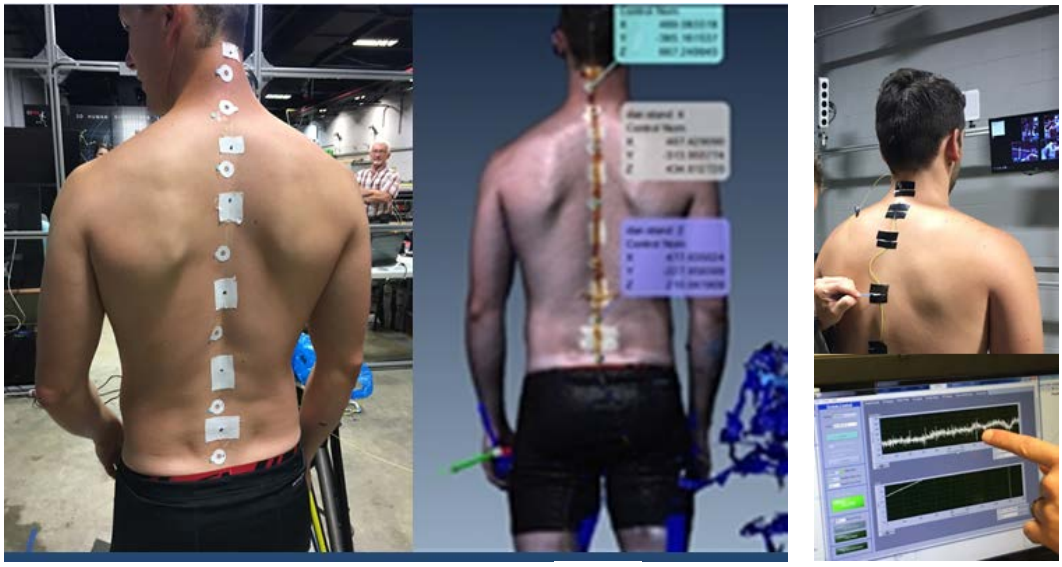

(a) (b) (c)

Figure 14. Luna sensor evaluation conducted with 3DMD whole body scanner. (a) Subject fit with the fiber optic cable positioned along his spine. (b) Resulting textured scan image. (c) "Cold touch" technique used to identify seven anatomical locations along the fiber optic cable.

For each group of 50 logged shape measurements, an average shape was computed. Prior to averaging, each of the 50 scans was evaluated using Luna's internal data quality metric. Only scans whose data quality metric was below the default threshold of 0.16 were included in the average. Over the 9 data sets collected, between 42 and 50 scans were included in each average. As an example, the data quality plot for posture 5 (46 out of 50 valid scans) is shown in Figure 15.

For each posture, the averaged X,Y,Z shape data were output to a .csv file for analysis. The .csv file format is shown in Table 2. The recorded data are decimated to an output spatial resolution of $1/10^{th}$ the system's native resolution: 0.8 mm per point.

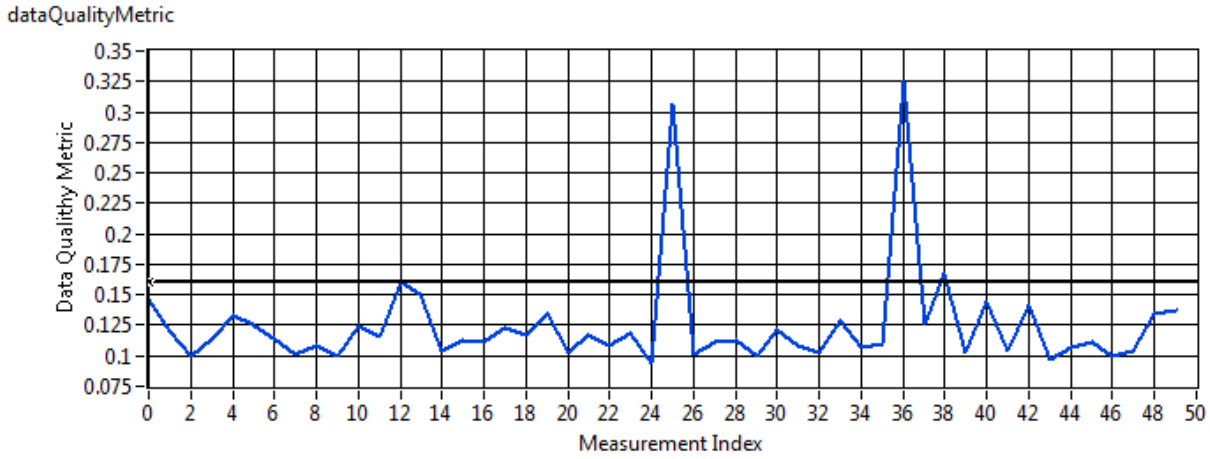

Figure 15. Example of a data quality plot for the subject's posture.

Table 2. An Example of a .csv File Used as Output from the Luna Sensor for One Posture

X (mm)	Y (mm)	Z (mm)
1.61596E-11	-5.61365E-12	8.04542E-2
1.13895E-9	-2.15751E-10	8.84996E-1
...	...	...
N = 2016 total values	N = 2016 total values	N = 2016 total values

Polyworks was used to evaluate the Luna sensor output shape versus the 3DMD whole body spine posture. Raw data are found in the Appendix. Summary results of the evaluation from the subject given various postures are found in Table 3. Selecting points from the 3DMD using Polyworks, coordinate data of the landmarks along the spine measured by the Luna system versus the 3DMD correlated best when the subject was standing straight without any leaning or torsion. The mean distance from the coordinates measured by 3DMD versus Luna is 1.9 mm. The mean distance for leaning left and leaning right is 2.2 mm and 2.0 mm, respectively. The mean distance for leaning forward is 3.1 mm. The mean distance for twisting left and twisting right is 3.3 mm and 3.8 mm, respectively. All of the distances between the points measured using the 3DMD system versus those measured by the Luna sensor fall within the tolerance of the point picking method given that the spread of color along the pixels representing the "point" covers approximately 5-6 mm of surface area. Therefore, the mean values for the difference measurements fall within the tolerance of the 3DMD scanning and image processing assessment. Ultimately, a 5- to 6-mm difference in vertebral position for an avatar modeled within RAMSIS is within subject positioning tolerance.

Table 3. Results of the Coordinate Data Extracted from 3DMD Scans Using Polyworks vs. the Luna Sensor Output

Posture	Distance Between Points Along Spine (in mm) from 3DMD and Luna							Mean
	1	2	3	4	5	6	7	
Twist right 1	3.9	3.3	2.8	2.4	4.4	4.9	2.6	
Twist right 2	3.7	4.4	3.7	2.4	4.0	5.1	1.3	
Twist right 3	6.0	4.9	3.7	2.8	4.5	7.0	1.8	
Mean	**4.5**	**4.2**	**3.4**	**2.5**	**4.3**	**5.7**	**1.9**	**3.8**
Twist left 1	1.4	2.3	1.0	1.6	3.8	4.3	3.2	
Twist left 2	5.1	4.0	0.9	2.9	3.4	5.1	1.7	
Twist left 3	4.7	4.8	2.3	2.6	5.1	6.4	2.2	
Mean	**3.7**	**3.7**	**1.4**	**2.4**	**4.1**	**5.3**	**2.4**	**3.3**
Standing straight 1	1.6	0.5	2.0	1.4	1.1	2.6	4.0	
Standing straight 2	2.2	1.0	2.4	1.2	1.6	2.6	2.6	
Standing straight 3	1.5	1.0	2.3	1.1	1.3	3.0	3.6	
Mean	**1.8**	**0.8**	**2.2**	**1.2**	**1.3**	**2.7**	**3.4**	**1.9**
Lean right 1	1.2	0.9	1.2	1.6	1.8	2.0	4.6	
Lean right 2	1.0	0.3	1.8	1.1	1.7	2.8	3.8	
Lean right 3	1.7	0.9	3.3	0.4	1.5	3.0	4.8	
Mean	**1.3**	**0.7**	**2.1**	**1.0**	**1.7**	**2.6**	**4.4**	**2.0**
Lean left 1	0.8	2.2	2.0	1.5	1.4	3.1	5.2	
Lean left 2	1.9	1.0	2.1	0.9	2.0	4.0	4.5	
Lean left 3	1.1	1.0	1.1	0.9	2.5	2.6	4.0	
Mean	**1.3**	**1.4**	**1.7**	**1.1**	**2.0**	**3.2**	**4.6**	**2.2**
Lean forward 1	2.1	1.7	2.3	1.9	2.3	4.1	2.8	
Lean forward 2	3.6	4.0	0.9	2.2	3.9	4.8	2.5	
Lean forward 3	5.0	4.9	1.8	3.0	4.1	5.7	1.3	
Mean	**3.6**	**3.5**	**1.7**	**2.3**	**3.4**	**4.9**	**2.2**	**3.1**
Mean	2.7	2.3	2.1	1.7	2.8	4.0	3.2	**2.7**
Standard deviation	1.6	1.7	0.8	0.8	1.3	1.4	1.2	**1.3**
Minimum	0.8	0.3	0.9	0.4	1.1	2.0	1.3	**1.0**
Maximum	6.0	4.9	3.7	3.0	5.1	7.0	5.2	**5.0**

Note: The mean differences fall within tolerances for modeling spine posture and position.

3.6.3 Evaluation Using Human Solutions VITUS Whole Body Scanner. The ability to implement Luna's single fiber optic cable to capture spine posture and position with a seated subject was demonstrated while subjects were encumbered and restrained in ejection seats. A collaborative effort between the USAF AE team and anthropometrists from the Naval Air Systems Command (NAVAIR) provided the opportunity to capture subjects with both USAF and NAVAIR AFE in a variety of ejection seats. These data are to be used as input to both the USAF and NAVAIR DHM systems to create models representing variability in size, position, and posture. As shown in Figure 16**,** the subjects were first instrumented with the Luna system, securing the fiber optic cable along the spine with medical grade tape. The bottom of the cable was located at the lumbar-sacrum joint, and the RAMSIS joint locations, as depicated in Figure 10, were measured and identified along the spine. At each RAMSIS joint location, the "cold touch" method revealed the corresponding point along the Luna cable. The coordinate reference box, shown in Figure 11b, was mounted on the ejection seat to provide data acquisition and a standard reference frame. The subjects were both encumbered and restrained. The ejection

seat, subject, and Luna acquisition system were located within the VITUS whole body scanner [10]. Shown in the lower right corner is the VITUS 3D scan of the subject in the ejection seat with the Luna position data aligned using the coordinate reference box. The addition of the Luna system provides improved biofidelic torso position data, particularly for potential initial ejection posture.

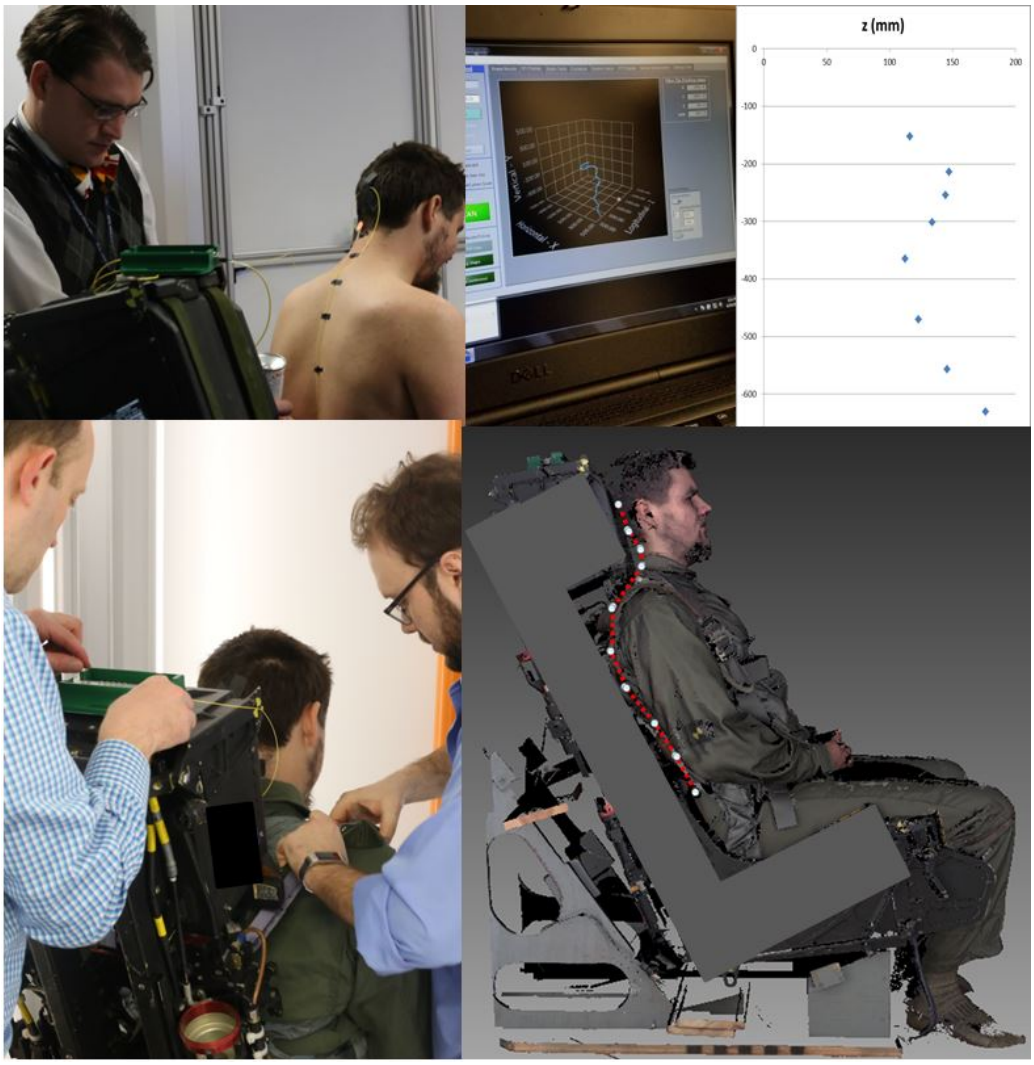

Figure 16. Implementation of Luna system to capture initial posture. Shown in the upper left corner, the subject is "fit" with the Luna system, identifying RAMSIS joint locations using the "cold touch" method. Shown in the upper right corner, the Luna positioning system is displayed in real time. In the lower left corner, the coordinate reference box is mounted to the ejection seat with the subject both encumbered and restrained. Shown in the right corner is the VITUS 3D scan of the subject in the ejections seat with the Luna position data aligned using the coordinate reference box.

4.0 RESULTS AND DISCUSSION

Application of the Luna positioning sensor to capture spine posture and position accurately for the purpose of DHM has been proven to be effective. The Luna system was evaluated on human subjects using both the Artec Eva handheld scanner and 3DMD whole body scanner. The subjects were tested with and without body armor, and the Luna system performed exceptionally. Measurement of the spine's posture by the Luna system is well within the tolerance for modeling the human body while standing or bending the spine, including as a seated subject. Coordinate data extracted from the 3DMD scans were compared to the positions of identical points along the spine recorded using the Luna system. The RAMSIS NextGen DHM is not programmed to automatically input vertebral locations from the human spine to the model. The model's spine orientation engine was studied to determine the most direct method of inputting the Luna data. Development of the RAMSIS digital manikins proved to be more problematic than originally considered. However, after working with Human Solutions to correct the anthropometric engine, the manikins duplicated the input dimensions. Given the corrected manikins, an approach to estimate vertebral element locations was determined for the RAMSIS models. This skeletal model can now be correlated directly with Luna positional data to determine spine orientation. This approach was tested using subjects encumbered and restrained within ejection seats while wearing the Luna fiber optic cable. A VITUS 3D scan of the subject was co-aligned with the spine posture data to capture both posture surface data and spine orientation.

5.0 CONCLUSION

In related research, the Anthropometry Lab is collaborating with the US Army Natick Soldier Research, Development and Engineering Center to develop a parametric 3D cervical spine model, beginning by extracting cervical measurements from planar X-rays to ultimately estimating head, neck, and shoulder shape and orientation given covariate subject information (stature, age, gender, etc.). Changes in neck orientation and position will be determined for a variety of subjects given differing helmet-mounted mass configurations (e.g., CG forward vs. in line with human head CG). These spine orientations will be used to establish load-bearing postures as a function of mass, subject parameters, and seated postures, as these will affect neck posture as well. The resulting models will improve the estimates of resultant head and neck loading in the ejection seat environment.

Development of workstation models with appropriate crew member database representation, digital accommodations, and spine orientation data using the Luna positioning sensor within the RAMSIS NextGen modeling environment provides a cost-efficient method to visualize and analyze workstation accommodation. The proposed approach supports a life cycle tool that will significantly reduce cost and time required for on-site measurement studies. By using a validated DHM system (RAMSIS NextGen), a number of system designs or modifications can be quickly assessed for safety, mission effectiveness, and occupational health. When using test participants, costs associated with travel, contract labor, and logistics are extensive as well, whereas evaluations based on validated modeling of the same designs or modifications will reduce time and costs once we have developed an accurate posture model for our digital, biofidelic anthropometric accommodation method.

6.0 REFERENCES

1. Zehner GF, Hudson JA. Body size accommodation in USAF aircraft. Wright-Patterson AFB (OH): Air Force Research Laboratory, Human Effectiveness Directorate; 2002. Technical Report AFRL-HE-WP-TR-2002-0118.
2. Hudson JA, Oudenhuijzen A, Zehner GF. Digital human modelling systems: a procedure for verification and validation using the F-16 crew station. Proceedings of the Human Factors and Ergonimics Society Annual Meeting. 2000; 44(38):723-726.
3. Reed MP, Flannagan CA. Anthropometric and postural variability: limitations of the boundary manikin approach. SAE International Journal of Passenger Cars-Mechanical Systems. 2000; 109:2247-2252. Technical Paper No. 2000-01-2172.
4. Loczi J, Dietz M, Nielson G. Validation and application of the 3-D CAD manikin RAMSIS in automotive design. Paper presented at the SAE International Congress and Exposition; 1999 Mar 1-4; Detroit, MI. Warrendale (PA): Society of Automotive Engineers; 1999. SAE Technical Paper 1999-01-1270.
5. Nemeth KJ, Ianni JD, Wampler JL. A comparison of virtual & live human standing reach. Wright-Patterson AFB (OH): Air Force Research Laboratory, Human Effectiveness Directorate; 1998. Technical Report AFRL-HE-WP-TR-1999-0227.
6. Kaibel J, Kubbat W, Albert O, Balzulat J, Seitz T. Posture prediction model for pilots in cockpits and the appliance on the human model RAMSIS. VDI/SAE International Conference on Digital Human Modeling for Design and Engineering. Munich, Germany; 2002. VDI-Berichte No. 1675.
7. Park JW, Jung KY, Chang JH, Kwon JU, You HC. Evaluation of driving posture prediction in digital human simulation using RAMSIS®. Proceedings of the Human Factors and Ergonomics Society Annual Meeting. 2011; 55(1):1711-1715.
8. Meindl RS, Hudson JA, Zehner GF. A multivariate anthropometric method for crew station design. Wright-Patterson AFB (OH): Armstrong Laboratory, Crew Systems Directorate; 1993. Technical Report AL-TR-1993-0054.
9. Zehner GF, Meindl RS, Hudson JA. A multivariate anthropometric method for crew station design: abridged. Wright-Patterson AFB (OH): Armstrong Laboratory, Crew Systems Directorate; 1993. Technical Report AL-TR-1992-0164.
10. Human Solutions. RAMSIS NextGen: the new approach to vehicle ergonomics. (n.d.). [Accessed 26 Apr 2018]. Available from https://www.human-solutions.com/mobility/front_content.php?idcat=774&lang=8.

APPENDIX
Results of 3DMD Evaluation of Luna Positioning Sensor

		Subj1		**TWIST RIGHT 3**										
			SCAN				LUNA				DELTA			DISTANCE
		x	y	z		x	y	z		x	y	z		
1	Bottom	18.44	259.08	-139.97		17.41	264.63	-138.03		-1.04	5.55	1.95		5.98
2		4.74	338.24	-110.64		3.34	342.52	-108.84		-1.40	4.28	1.80		4.85
3		-19.56	450.69	-71.19		-21.93	452.79	-69.29		-2.37	2.10	1.90		3.69
4		-56.37	564.49	-24.05		-56.69	561.68	-24.14		-0.32	-2.81	-0.09		2.83
5		-106.16	652.19	30.82		-104.11	648.28	29.80		2.05	-3.91	-1.02		4.53
6		-143.53	695.92	72.47		-140.11	692.41	67.46		3.42	-3.51	-5.01		7.01
7	Top	-186.49	729.37	106.28		-186.82	727.67	106.75		-0.33	-1.70	0.47		1.80
									ABSMean	0.00	0.00	0.00		4.38
									SD	2.03	3.92	2.48		1.79

		Subj1		**TWIST RIGHT 2**										
			SCAN				LUNA				DELTA			DISTANCE
		x	y	z		x	y	z		x	y	z		
1	Bottom	26.08	263.65	-153.42		26.30	267.02	-151.83		0.23	3.37	1.59		3.73
2		7.53	337.74	-119.55		5.98	341.62	-118.09		-1.55	3.88	1.46		4.43
3		-25.62	447.11	-74.88		-29.24	447.61	-74.61		-3.62	0.50	0.27		3.66
4		-75.38	554.18	-28.36		-75.06	551.84	-28.34		0.32	-2.35	0.02		2.37
5		-134.26	636.17	25.82		-132.09	632.96	24.86		2.17	-3.21	-0.96		3.99
6		-176.64	676.10	64.01		-172.90	673.70	61.45		3.74	-2.41	-2.56		5.13
7	Top	-220.41	710.36	95.69		-221.70	710.58	95.87		-1.29	0.21	0.18		1.32
									Mean	0.00	0.00	0.00		3.52
									SD	2.45	2.84	1.43		1.28

		Subj1		**TWIST RIGHT 1**										
			SCAN				LUNA				DELTA			DISTANCE
		x	y	z		x	y	z		x	y	z		
1	Bottom	30.74	260.44	-162.40		31.03	263.91	-160.62		0.29	3.47	1.78		3.92
2		17.62	337.81	-129.28		15.73	340.38	-128.49		-1.89	2.57	0.80		3.29
3		-9.64	447.65	-85.96		-12.14	448.73	-85.49		-2.50	1.08	0.47		2.76
4		-51.32	558.46	-39.89		-50.01	556.49	-40.03		1.31	-1.97	-0.13		2.37
5		-100.99	646.84	13.55		-98.34	643.47	12.53		2.64	-3.37	-1.02		4.40
6		-136.22	691.40	52.46		-134.37	688.85	48.68		1.84	-2.56	-3.78		4.92
7	Top	-177.34	730.35	80.94		-179.04	731.12	82.82		-1.70	0.77	1.88		2.65
									Mean	0.00	0.00	0.00		3.47
									SD	2.04	2.65	1.95		0.97

		Subj1		**TWIST LEFT 3**										
			SCAN				LUNA				DELTA			DISTANCE
		x	y	z		x	y	z		x	y	z		
1	Bottom	-55.89	266.92	-186.13		-53.78	270.82	-184.52		2.10	3.90	1.61		4.72
2		-42.33	343.48	-153.70		-40.65	347.50	-151.67		1.68	4.01	2.03		4.80
3		-11.26	451.95	-104.34		-12.40	453.00	-102.59		-1.15	1.05	1.75		2.34
4		27.07	558.64	-47.88		26.19	556.19	-48.11		-0.88	-2.45	-0.23		2.61
5		75.52	642.01	12.65		77.02	638.56	9.23		1.49	-3.45	-3.42		5.09
6		120.99	683.58	49.29		116.70	680.55	45.59		-4.29	-3.03	-3.70		6.42
7	Top	160.79	715.72	84.27		161.83	715.68	86.23		1.04	-0.04	1.96		2.22
									Mean	0.00	0.00	0.00		4.03
									SD	2.28	3.15	2.55		1.64

		Subj1		**TWIST LEFT 2**										
			SCAN				LUNA				DELTA			DISTANCE
		x	y	z		x	y	z		x	y	z		
1	Bottom	-76.79	265.00	-187.22		-74.72	269.23	-185.34		2.07	4.24	1.88		5.08
2		-63.46	342.85	-154.86		-63.30	346.24	-152.68		0.16	3.40	2.19		4.04
3		-41.20	452.60	-103.25		-41.72	452.88	-102.59		-0.53	0.28	0.67		0.90
4		-11.55	560.74	-45.42		-11.49	558.31	-47.07		0.06	-2.44	-1.65		2.94
5		31.48	646.50	13.76		31.98	643.50	12.22		0.51	-3.00	-1.54		3.41
6		70.93	690.35	52.77		67.25	687.80	50.34		-3.68	-2.54	-2.43		5.09
7	Top	106.02	725.98	92.05		107.42	726.05	92.93		1.41	0.07	0.88		1.66
									Mean	0.00	0.00	0.00		3.30
									SD	1.84	2.91	1.85		1.61

		Subj1		**TWIST LEFT 1**										
			SCAN				LUNA				DELTA			DISTANCE
		x	y	z		x	y	z		x	y	z		
1	Bottom	-54.41	264.23	-218.58		-54.06	265.62	-218.51		0.35	1.39	0.07		1.43
2		-41.92	339.55	-184.71		-41.89	341.57	-183.67		0.03	2.02	1.04		2.27
3		-15.15	445.83	-133.26		-14.89	446.34	-132.40		0.25	0.52	0.87		1.04
4		19.82	554.41	-82.03		20.03	552.87	-81.76		0.20	-1.54	0.26		1.58
5		65.77	644.83	-29.96		67.18	642.37	-32.45		1.41	-2.45	-2.49		3.77
6		107.28	692.46	1.10		103.98	690.02	-0.29		-3.29	-2.44	-1.39		4.33
7	Top	138.53	735.67	34.72		139.58	738.18	36.35		1.05	2.52	1.63		3.18
									Mean	0.00	0.00	0.00		2.51
									SD	1.54	2.12	1.46		1.26

		Subj1		**Standing Straight 3 (Initial 3)**										
			SCAN				LUNA				DELTA			DISTANCE
		x	y	z		x	y	z		x	y	z		
1	Bottom	-26.54	225.42	-181.37		-25.86	224.99	-182.62		0.68	-0.43	-1.25		1.48
2		-25.34	305.74	-163.36		-24.67	305.80	-162.65		0.68	0.06	0.71		0.98
3		-21.29	422.59	-148.78		-22.97	423.88	-148.00		-1.67	1.29	0.78		2.25
4		-20.61	546.93	-145.08		-21.43	546.23	-144.82		-0.83	-0.70	0.26		1.12
5		-18.17	658.94	-131.70		-17.32	657.92	-131.54		0.85	-1.02	0.16		1.34
6		-11.60	725.54	-111.06		-11.91	722.89	-112.36		-0.30	-2.65	-1.30		2.97
7	Top	-11.08	784.73	-97.69		-10.49	788.17	-97.05		0.59	3.45	0.64		3.56
									Mean	0.00	0.00	0.00		1.96
									SD	0.96	1.93	0.90		0.99

		Subj1		**Standing Straight 2 (Initial 2)**										
			SCAN				LUNA				DELTA			DISTANCE
		x	y	z		x	y	z		x	y	z		
1	Bottom	-49.11	226.41	-192.23		-47.93	228.28	-192.36		1.17	1.88	-0.13		2.22
2		-46.46	308.29	-170.33		-46.05	308.47	-171.22		0.41	0.18	-0.89		1.00
3		-39.04	426.75	-159.28		-41.17	426.72	-158.27		-2.13	-0.03	1.02		2.36
4		-36.10	549.76	-156.68		-36.69	549.24	-155.80		-0.60	-0.52	0.88		1.19
5		-30.04	662.13	-141.20		-29.48	660.58	-141.03		0.56	-1.54	0.17		1.65
6		-20.93	727.64	-121.26		-20.70	725.12	-121.93		0.23	-2.52	-0.67		2.62
7	Top	-18.37	788.54	-108.68		-18.01	791.10	-109.06		0.36	2.56	-0.38		2.61
									Mean	0.00	0.00	0.00		1.95
									SD	1.07	1.78	0.73		0.67

		Subj1		**Standing Straight 1 (Initial 1)**										
			SCAN				LUNA				DELTA			DISTANCE
		x	y	z		x	y	z		x	y	z		
1	Bottom	-41.14	225.77	-174.16		-39.82	225.37	-174.97		1.32	-0.40	-0.81		1.60
2		-38.60	305.02	-151.94		-38.59	304.87	-152.39		0.02	-0.15	-0.44		0.47
3		-33.17	422.88	-140.41		-34.65	423.25	-139.17		-1.48	0.37	1.23		1.96
4		-30.57	546.13	-139.71		-31.80	545.94	-139.14		-1.22	-0.20	0.58		1.37
5		-27.20	658.68	-126.27		-26.98	657.65	-126.33		0.22	-1.04	-0.06		1.06
6		-20.27	725.05	-107.64		-19.75	722.55	-107.82		0.52	-2.51	-0.18		2.57
7	Top	-18.97	784.39	-94.27		-18.35	788.31	-94.59		0.62	3.92	-0.32		3.98
									Mean	0.00	0.00	0.00		1.86
									SD	1.01	1.96	0.69		1.15

		Subj1		**Lean Right 3**										
			SCAN				LUNA				DELTA			DISTANCE
		x	y	z		x	y	z		x	y	z		
1	Bottom	-31.48	230.99	-189.56		-29.83	230.91	-189.70		1.65	-0.07	-0.14		1.66
2		-30.70	310.57	-168.94		-30.17	311.29	-168.67		0.53	0.72	0.27		0.93
3		-42.69	427.75	-150.19		-45.64	426.34	-150.09		-2.95	-1.41	0.10		3.27
4		-84.95	541.17	-142.30		-84.87	541.09	-142.67		0.09	-0.09	-0.37		0.39
5		-129.06	644.04	-122.86		-127.98	643.11	-123.27		1.09	-0.93	-0.42		1.49
6		-151.88	705.47	-100.34		-152.41	702.76	-101.52		-0.53	-2.71	-1.17		3.00
7	Top	-184.97	755.53	-89.09		-184.85	760.01	-87.37		0.11	4.49	1.73		4.81
									Mean	0.00	0.00	0.00		2.22
									SD	1.48	2.27	0.89		1.54

		Subj1		**Lean Right 2**										
			SCAN				LUNA				DELTA			DISTANCE
		x	y	z		x	y	z		x	y	z		
1	Bottom	-44.84	229.87	-196.41		-44.15	230.37	-195.97		0.69	0.50	0.44		0.96
2		-44.32	310.76	-175.05		-44.02	310.72	-175.11		0.30	-0.04	-0.06		0.31
3		-57.27	426.22	-156.04		-59.05	425.90	-156.33		-1.78	-0.32	-0.30		1.83
4		-97.35	539.90	-148.27		-97.24	539.53	-149.25		0.11	-0.37	-0.98		1.06
5		-141.26	641.85	-132.60		-139.72	641.20	-132.21		1.53	-0.65	0.39		1.71
6		-164.04	705.27	-112.51		-163.69	702.56	-112.15		0.35	-2.71	0.36		2.75
7	Top	-193.94	758.08	-100.52		-195.14	761.67	-100.36		-1.20	3.59	0.16		3.79
									Mean	0.00	0.00	0.00		1.77
									SD	1.13	1.88	0.51		1.18

		Subj1		**Lean Right 1**										
			SCAN				LUNA				DELTA			DISTANCE
		x	y	z		x	y	z		x	y	z		
1	Bottom	-38.84	230.31	-185.56		-38.07	229.42	-185.50		0.77	-0.90	0.06		1.18
2		-37.67	310.48	-165.52		-38.18	309.93	-165.01		-0.51	-0.56	0.51		0.91
3		-48.59	426.88	-149.27		-49.68	427.08	-149.70		-1.09	0.19	-0.43		1.19
4		-82.09	543.78	-146.84		-81.25	543.33	-148.11		0.84	-0.45	-1.27		1.59
5		-118.68	648.95	-133.08		-116.94	648.68	-132.77		1.73	-0.27	0.31		1.78
6		-137.45	713.26	-115.35		-136.62	711.49	-115.31		0.83	-1.77	0.04		1.95
7	Top	-162.68	769.00	-108.77		-165.25	772.75	-107.99		-2.57	3.75	0.78		4.61
									Mean	0.00	0.00	0.00		1.89
									SD	1.48	1.76	0.68		1.26

		Subj1		**Lean Left 3**										
			SCAN				LUNA				DELTA			DISTANCE
		x	y	z		x	y	z		x	y	z		
1	Bottom	-57.66	233.34	-174.94		-56.64	233.72	-174.77		1.03	0.37	0.18		1.10
2		-52.77	312.77	-150.26		-52.91	313.70	-150.69		-0.13	0.93	-0.43		1.03
3		-31.82	428.09	-131.31		-32.65	428.67	-130.84		-0.82	0.58	0.47		1.11
4		14.47	541.73	-123.88		14.17	540.84	-123.93		-0.30	-0.89	-0.05		0.95
5		69.03	640.34	-106.76		68.72	637.83	-106.94		-0.31	-2.51	-0.17		2.54
6		108.40	691.50	-84.24		106.35	690.07	-84.94		-2.05	-1.43	-0.70		2.59
7	Top	141.24	741.22	-70.42		143.83	744.18	-69.71		2.60	2.96	0.71		4.00
									Mean	0.00	0.00	0.00		1.90
									SD	1.47	1.79	0.49		1.17

		Subj1		**Lean Left 2**										
			SCAN				LUNA				DELTA			DISTANCE
		x	y	z		x	y	z		x	y	z		
1	Bottom	-63.39	231.35	-175.94		-62.09	232.70	-175.64		1.30	1.35	0.30		1.90
2		-59.47	312.87	-149.87		-58.97	312.42	-150.57		0.50	-0.46	-0.70		0.97
3		-39.36	427.17	-131.55		-41.22	427.25	-130.63		-1.86	0.08	0.92		2.08
4		3.19	540.16	-127.34		2.56	540.69	-127.59		-0.63	0.52	-0.25		0.85
5		55.03	639.98	-112.77		55.38	638.11	-113.33		0.36	-1.87	-0.56		1.99
6		96.78	693.53	-94.79		93.64	691.11	-94.70		-3.14	-2.42	0.09		3.96
7	Top	126.99	744.23	-83.46		130.46	747.03	-83.26		3.47	2.79	0.20		4.46
									Mean	0.00	0.00	0.00		2.32
									SD	2.15	1.80	0.55		1.39

		Subj1		**Lean Left 1**										
			SCAN				LUNA				DELTA			DISTANCE
		x	y	z		x	y	z		x	y	z		
1	Bottom	-52.12	231.87	-185.64		-52.09	231.34	-186.18		0.02	-0.54	-0.54		0.76
2		-51.16	313.66	-162.38		-50.55	311.52	-162.18		0.60	-2.14	0.20		2.23
3		-30.97	425.82	-141.77		-32.97	426.09	-141.49		-2.01	0.27	0.29		2.05
4		11.43	536.43	-136.03		11.19	537.73	-136.72		-0.25	1.29	-0.69		1.49
5		64.56	635.60	-121.19		65.40	634.54	-120.95		0.85	-1.06	0.24		1.38
6		106.46	688.76	-101.75		104.09	686.78	-101.37		-2.38	-1.98	0.38		3.11
7	Top	138.07	737.68	-89.40		141.23	741.84	-89.29		3.16	4.15	0.12		5.22
									Mean	0.00	0.00	0.00		2.32
									SD	1.86	2.19	0.43		1.48

		Subj1		**Lean Forward 3**										
			SCAN				LUNA				DELTA			DISTANCE
		x	y	z		x	y	z		x	y	z		
1	Bottom	-27.87	263.96	-198.92		-27.81	268.62	-196.99		0.06	4.66	1.93		5.05
2		-25.82	342.06	-166.61		-25.95	346.50	-164.49		-0.13	4.45	2.12		4.93
3		-24.26	455.68	-118.27		-23.98	456.36	-116.63		0.28	0.67	1.64		1.79
4		-23.07	567.88	-58.80		-22.93	564.91	-58.96		0.15	-2.97	-0.15		2.97
5		-21.21	656.39	13.17		-20.86	652.81	11.21		0.36	-3.58	-1.96		4.10
6		-16.33	700.11	67.74		-17.61	697.16	63.02		-1.28	-2.94	-4.72		5.71
7	Top	-16.67	734.37	121.82		-16.11	734.08	122.97		0.57	-0.29	1.15		1.32
									Mean	0.00	0.00	0.00		3.69
									SD	0.61	3.47	2.53		1.70

		Subj1		**Lean Forward 2**										
			SCAN				LUNA				DELTA			DISTANCE
		x	y	z		x	y	z		x	y	z		
1	Bottom	-29.40	261.45	-207.14		-29.24	264.80	-205.70		0.16	3.35	1.44		3.65
2		-27.76	340.66	-178.95		-27.87	344.31	-177.40		-0.10	3.65	1.55		3.97
3		-25.91	455.63	-134.49		-25.73	455.82	-133.65		0.18	0.19	0.83		0.87
4		-24.56	568.36	-79.46		-24.98	566.25	-79.68		-0.41	-2.11	-0.22		2.16
5		-22.62	659.30	-9.92		-21.87	656.15	-12.11		0.75	-3.15	-2.19		3.91
6		-16.66	705.71	41.30		-17.41	702.71	37.63		-0.75	-3.00	-3.67		4.80
7	Top	-16.35	744.35	91.29		-16.17	745.42	93.53		0.18	1.07	2.24		2.49
									Mean	0.00	0.00	0.00		3.12
									SD	0.48	2.86	2.18		1.34

		Subj1		**Lean Forward 1**										
			SCAN				LUNA				DELTA			DISTANCE
		x	y	z		x	y	z		x	y	z		
1	Bottom	-15.89	256.57	-214.41		-15.29	258.50	-213.94		0.60	1.92	0.47		2.07
2		-13.37	336.38	-186.14		-13.01	338.00	-185.74		0.36	1.62	0.40		1.71
3		-6.69	450.72	-149.77		-8.34	451.86	-148.63		-1.65	1.13	1.14		2.30
4		-4.93	569.87	-108.19		-4.77	567.98	-108.37		0.16	-1.89	-0.17		1.91
5		0.25	667.75	-52.36		1.09	665.87	-53.27		0.84	-1.88	-0.91		2.26
6		7.49	720.25	-6.23		7.42	717.76	-9.44		-0.07	-2.49	-3.21		4.06
7	Top	10.44	765.03	38.39		10.18	766.63	40.67		-0.25	1.59	2.29		2.80
									Mean	0.00	0.00	0.00		2.44
									SD	0.82	1.98	1.74		0.79

distance between points in mm from 3DMD and Luna								
Neal	bottom						top	
points along spine	**1**	**2**	**3**	**4**	**5**	**6**	**7**	
Twist right 1	3.9	3.3	2.8	2.4	4.4	4.9	2.6	
Twist right 2	3.7	4.4	3.7	2.4	4.0	5.1	1.3	
Twist right 3	6.0	4.9	3.7	2.8	4.5	7.0	1.8	
	4.5	**4.2**	**3.4**	**2.5**	**4.3**	**5.7**	**1.9**	**3.8**
Twist left 1	1.4	2.3	1.0	1.6	3.8	4.3	3.2	
Twist left 2	5.1	4.0	0.9	2.9	3.4	5.1	1.7	
Twist left 3	4.7	4.8	2.3	2.6	5.1	6.4	2.2	
	3.7	**3.7**	**1.4**	**2.4**	**4.1**	**5.3**	**2.4**	**3.3**
Standing straight 1	1.6	0.5	2.0	1.4	1.1	2.6	4.0	
Standing straight 2	2.2	1.0	2.4	1.2	1.6	2.6	2.6	
Standing straight 3	1.5	1.0	2.3	1.1	1.3	3.0	3.6	
	1.8	**0.8**	**2.2**	**1.2**	**1.3**	**2.7**	**3.4**	**1.9**
Lean right 1	1.2	0.9	1.2	1.6	1.8	2.0	4.6	
Lean right 2	1.0	0.3	1.8	1.1	1.7	2.8	3.8	
Lean right 3	1.7	0.9	3.3	0.4	1.5	3.0	4.8	
	1.3	**0.7**	**2.1**	**1.0**	**1.7**	**2.6**	**4.4**	**2.0**
Lean left 1	0.8	2.2	2.0	1.5	1.4	3.1	5.2	
Lean left 2	1.9	1.0	2.1	0.9	2.0	4.0	4.5	
Lean left 3	1.1	1.0	1.1	0.9	2.5	2.6	4.0	
	1.3	**1.4**	**1.7**	**1.1**	**2.0**	**3.2**	**4.6**	**2.2**
Lean forward 1	2.1	1.7	2.3	1.9	2.3	4.1	2.8	
Lean forward 2	3.6	4.0	0.9	2.2	3.9	4.8	2.5	
Lean forward 3	5.0	4.9	1.8	3.0	4.1	5.7	1.3	
	3.6	**3.5**	**1.7**	**2.3**	**3.4**	**4.9**	**2.2**	**3.1**
mean	2.7	2.3	2.1	1.7	2.8	4.0	3.2	**2.7**
std dev	1.6	1.7	0.8	0.8	1.3	1.4	1.2	**1.3**
min	0.8	0.3	0.9	0.4	1.1	2.0	1.3	**1.0**
max	6.0	4.9	3.7	3.0	5.1	7.0	5.2	**5.0**

LIST OF ABBREVIATIONS AND ACRONYMS

3D	three-dimensional
AE	anthropometric engineering
AFE	aircrew flight equipment
CAD	computer-aided design
CG	center of gravity
DHM	digital human modeling
JPATS	Joint Primary Aircraft Training System
JSF	Joint Strike Fighter
NAVAIR	Naval Air Systems Command
PCA	principal component analysis
USAF	U.S. Air Force